Addition of Monovalent Silver Cations to $CH_3NH_3PbBr_3$ Produces Crystallographically Oriented Perovskite Thin Films

Timothy D. Siegler,[†‡] Yangning Zhang,[†‡] Andrei Dolocan,[‡] Lauren R. Reimnitz,[†‡] Aida Torabi,[§] Michael Abney,[†‡] Junho Choi,[⊥] Gabriel Cossio,[‖] Daniel W. Houck,[†‡] Edward T. Yu,[‡‖] Xiaoqin Li,[‡⊥] Taylor Harvey,[§] Delia J. Milliron,[†‡] and Brian A. Korgel[†‡]*

[†]McKetta Department of Chemical Engineering, [‡]Texas Materials Institute, and [⊥]Department of Physics, Complex Quantum Systems, The University of Texas at Austin, Austin, Texas, 78712-1062

[§]Department of Science and Mathematics, Texas A&M University-Central Texas, Killeen, Texas, 76549

[‖]Microelectronics Research Center, Department of Electrical and Computer Engineering, The University of Texas at Austin, Austin, TX 78758

*corresponding author: korgel@che.utexas.edu

SUPPORTING INFORMATION

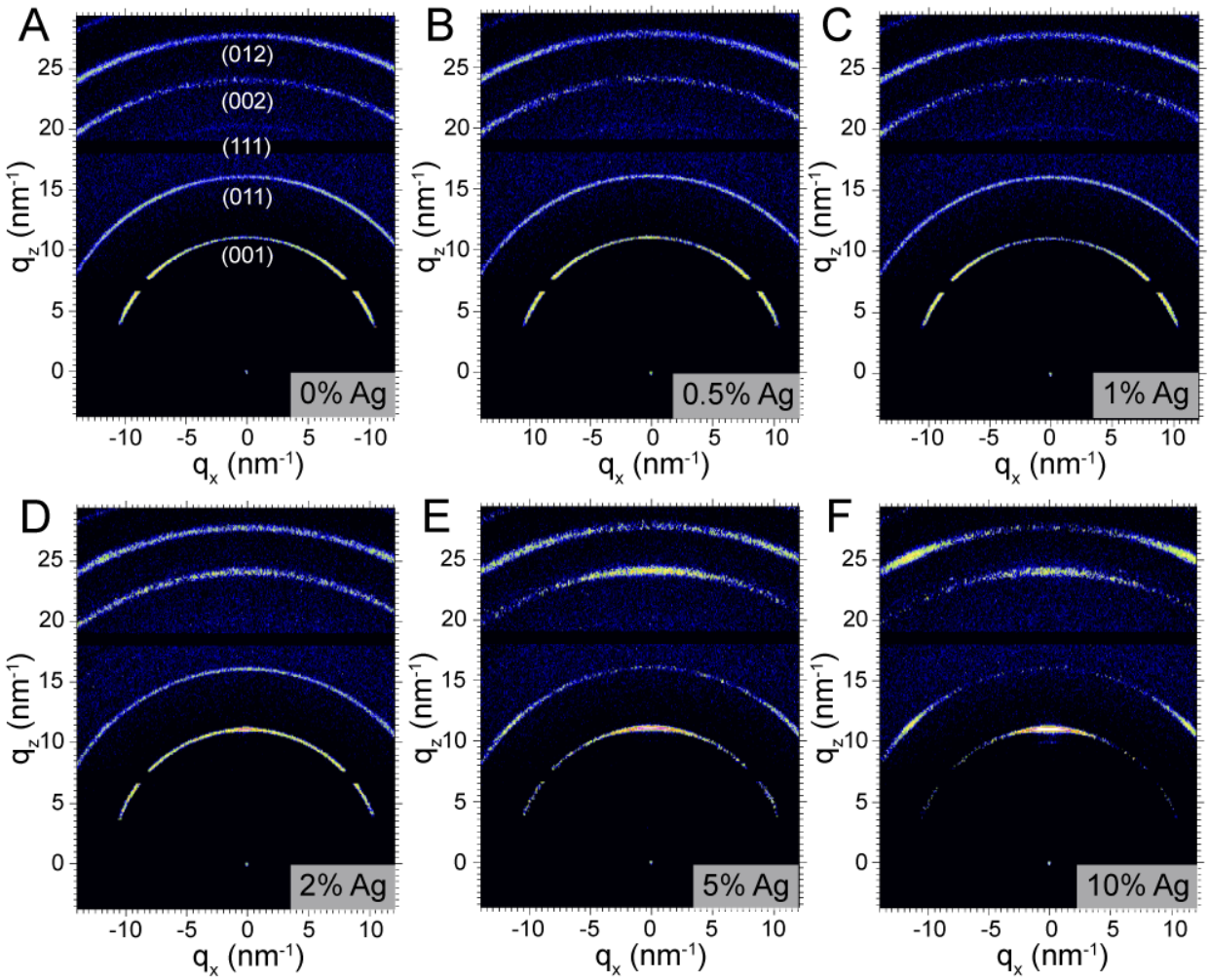

Figure S1. GIWAXS of MAPBr films deposited on glass substrates with varying amounts of Ag^+ added: (a) 0%, (b) 0.5%, (c) 1%, (d) 2%, (e) 5%, and (f) 10%. Diffraction patterns show weak (011) ordering in the absence of silver, which is replaced with an increasing degree of (001) ordering as silver is added to the MAPBr thin film.

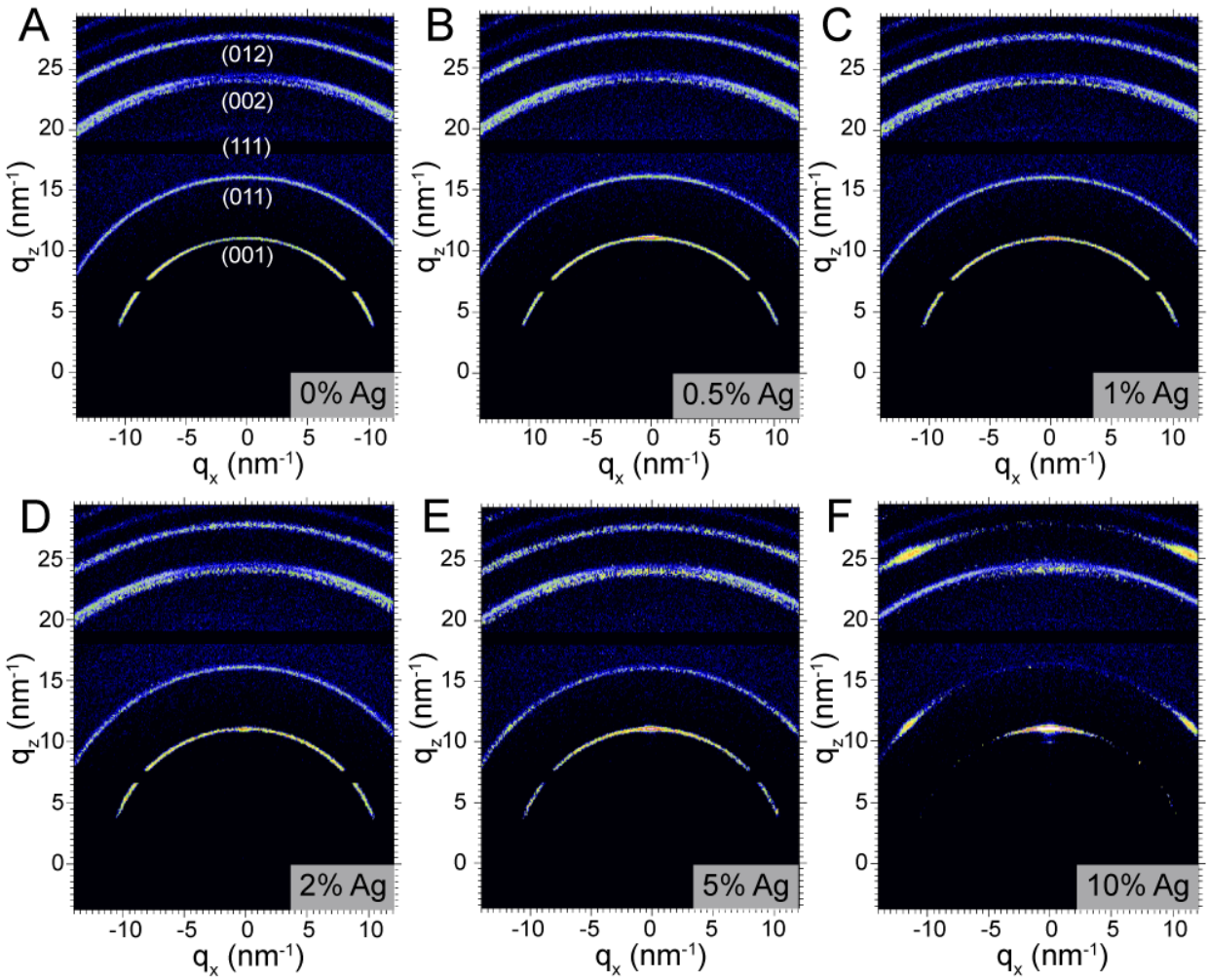

Figure S2. GIWAXS of MAPBr films on ITO-coated glass substrates with varying amounts of added Ag^+: (a) 0%, (b) 0.5%, (c) 1%, (d) 2%, (e) 5%, and (f) 10%. The diffraction patterns show a weak preference for (011) crystal orientation in the absence of Ag^+. Ag+ addition leads to films with (001) crystal orientation.

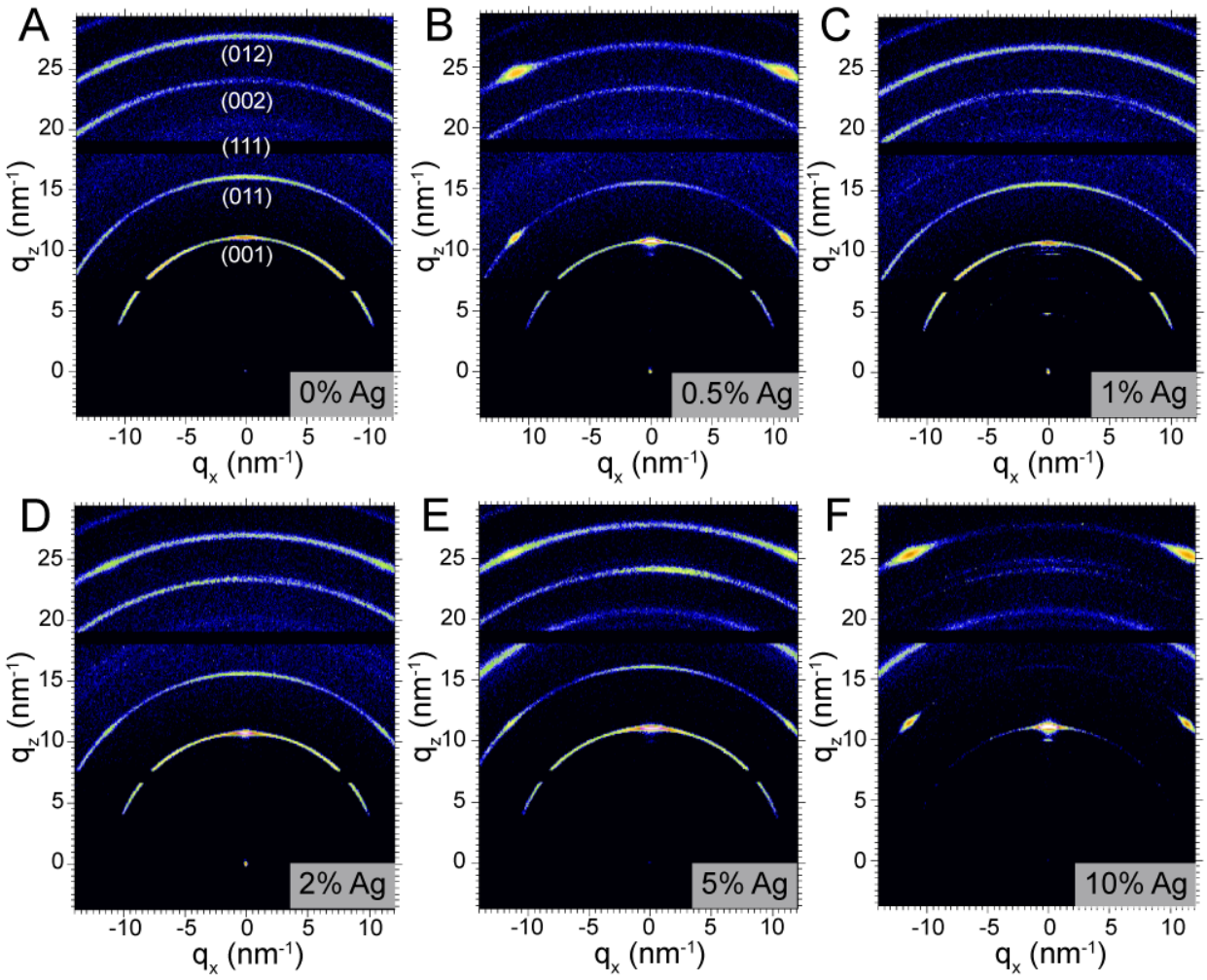

Figure S3. GIWAXS of MAPBr films on FTO-coated glass substrates with a ~50 nm compact TiO_2 layer, and a mesoporous TiO_2 layer with varying amounts of Ag^+ added: (a) 0%, (b) 0.5%, (c) 1%, (d) 2%, (e) 5%, and (f) 10%. As in Figure S2, the MAPBr diffraction patterns show a weak preference for (011) crystal orientation and then exhibit strongly preferred (001) crystal orientation with added Ag^+.

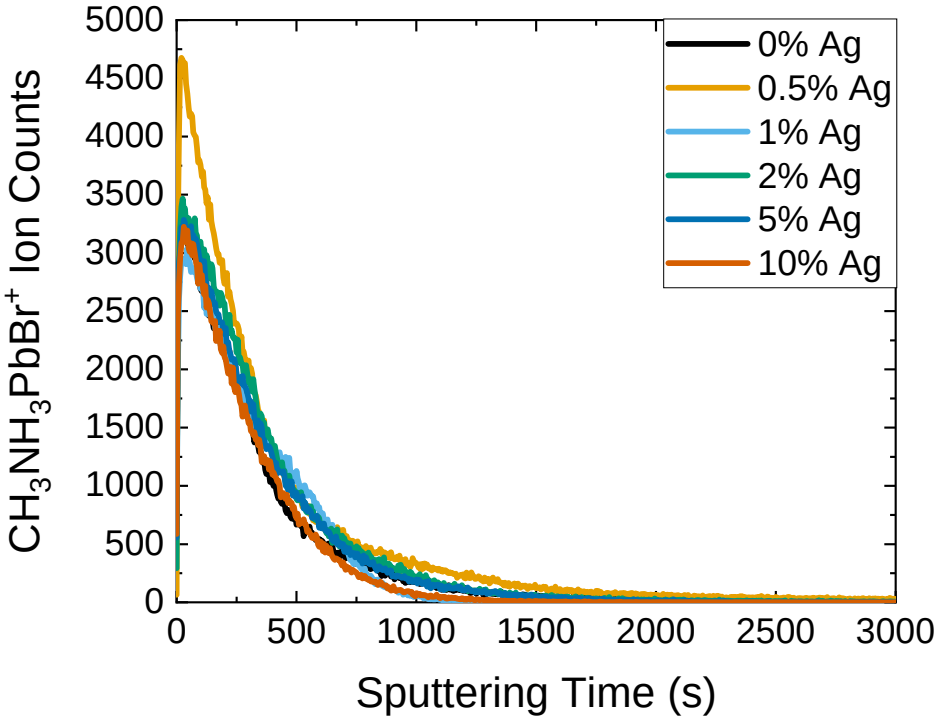

Figure S4. Plot of the absolute intensity of CH_3NH_3PbBr secondary ion fragment as a function of sputtering time for each sample shown in Figure 4b.

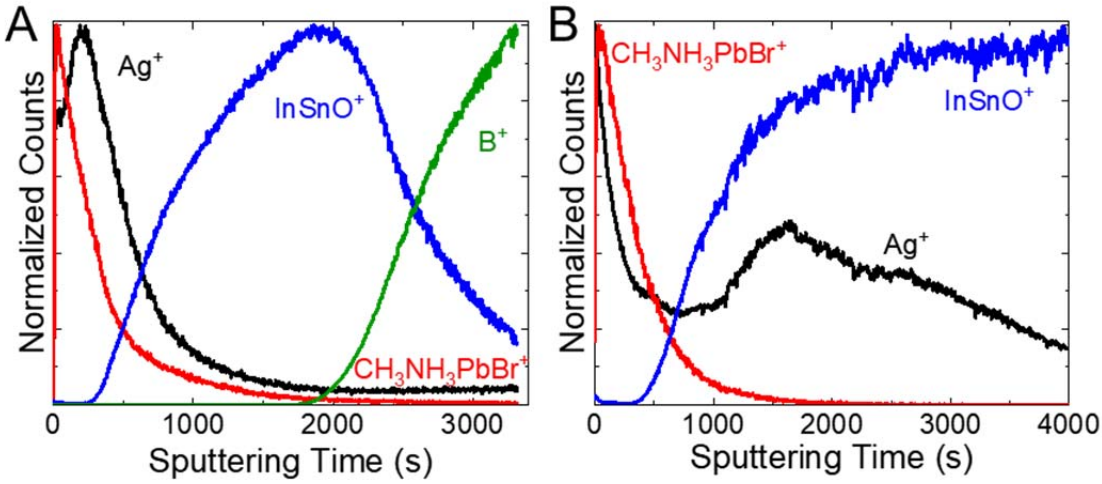

Figure S5. TOF-SIMS depth profiles of MAPBr films deposited with the addition of (A) 0.5% and (B) 5% Ag^+. The CH_3NH_3PbBr secondary ion fragment corresponds to the MAPBr layer, the Ag secondary ion fragment corresponds to silver, the InSnO secondary ion fragment to the ITO layer, and B secondary ion to borosilicate glass.

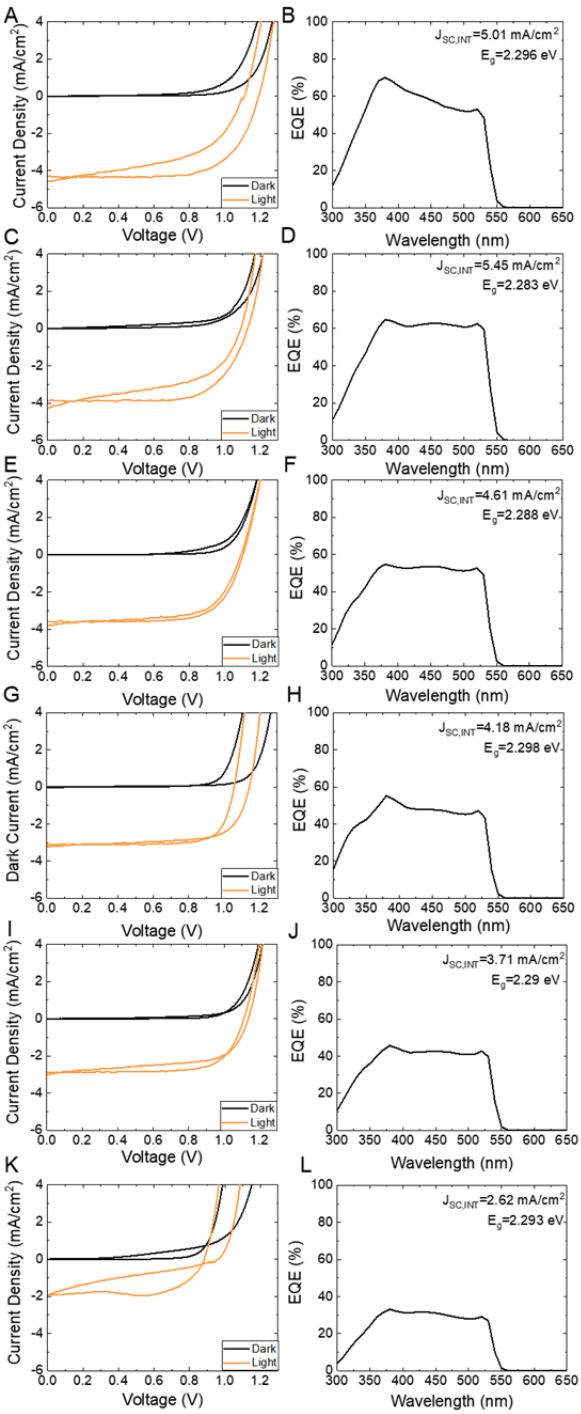

Figure S6. (A,C,E,G,I,K) *J-V* and (B,D,F,H,J,L) EQE data for representative Ag-MAPBr PV devices with (A-B) 0%, (C-D) 0.5%, (E-F) 1%, (G-H) 2%, (I-J) 5%, and (J-K) 10% Ag^{+}. The short circuit current (J_{SC}) obtained by integrating the EQE curves. EQE measurement consistently overestimates the J_{SC} values of the devices obtained from *J-V* curves, but are fairly consistent overall. Above 1% Ag^{+} incorporation, forward scans show higher V_{OC} than reverse scans.

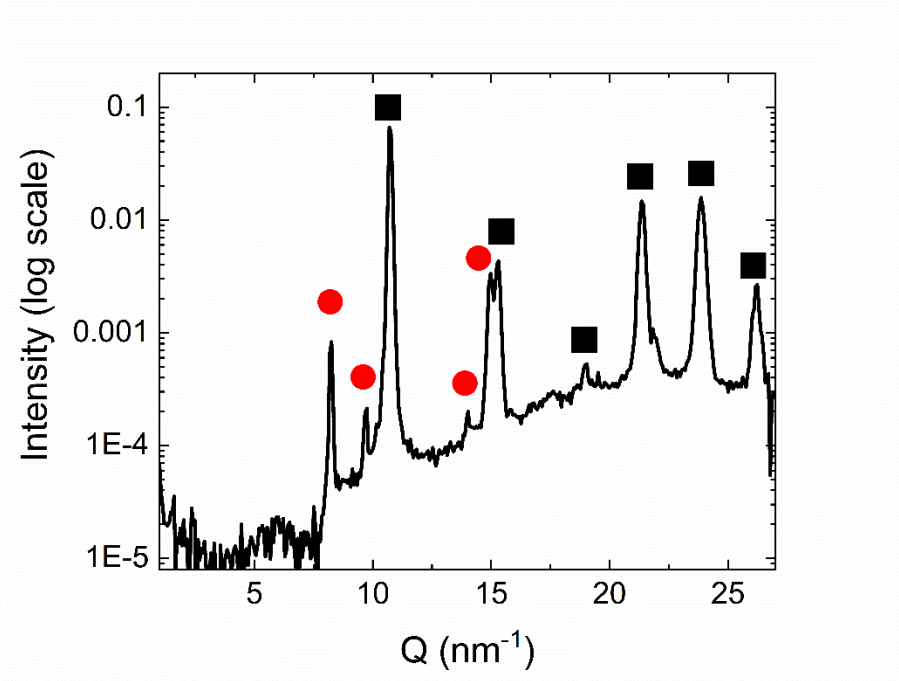

Figure S7. Azimuthally-integrated GIWAXS of MAPBr with 10% added Ag^+ with the impurity peaks marked with ● (MAPBr PDF #01-084-9476 is indexed by ■). These peaks most likely correspond to a material with the composition observed by TOF-SIMS of $Ag_xPb_yBr_{x+2y}$. The lattice spacing of the first unidentified peak is 7.76 Å.

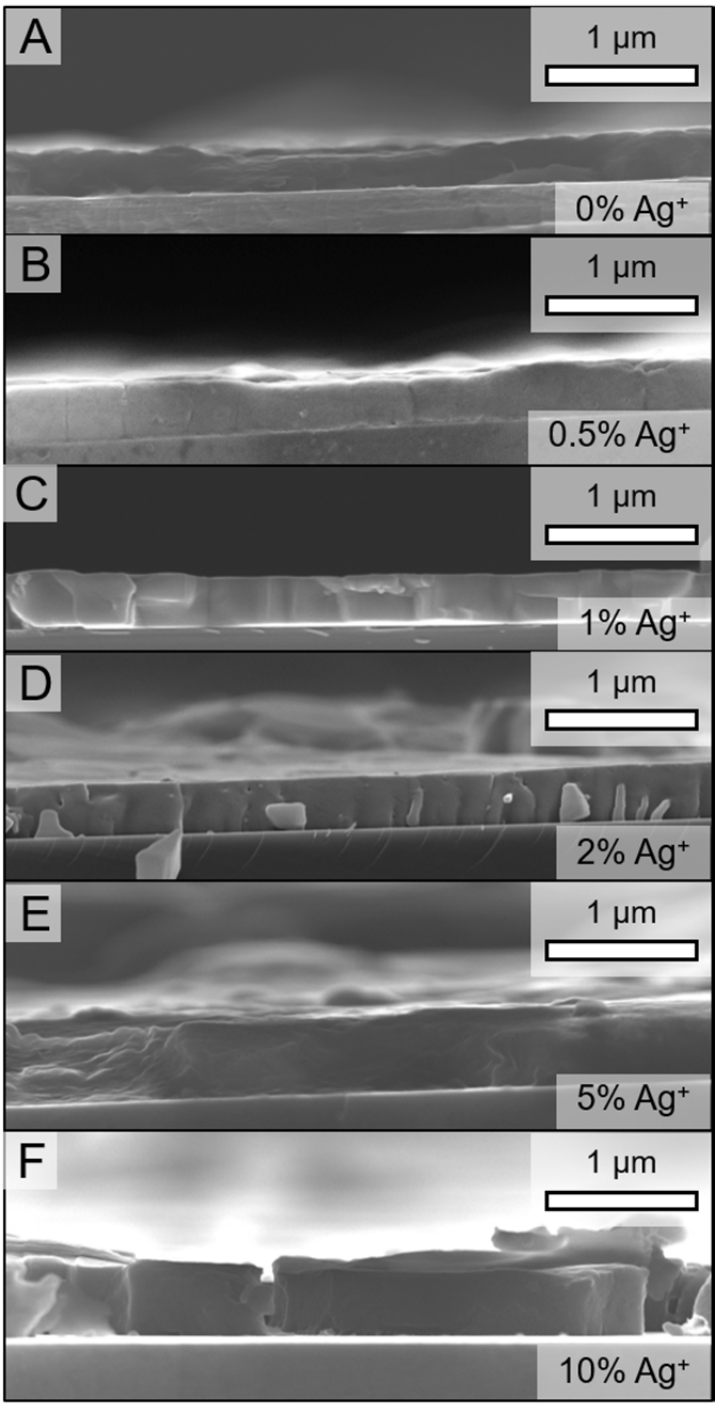

Figure S8. SEM images of cross-sectioned MAPBr films on silicon substrates that were deposited with the addition of (A) 0%, (B) 0.5%, (C) 1%, (D) 2%, (E) 5%, and (F) 10% Ag^{+}.

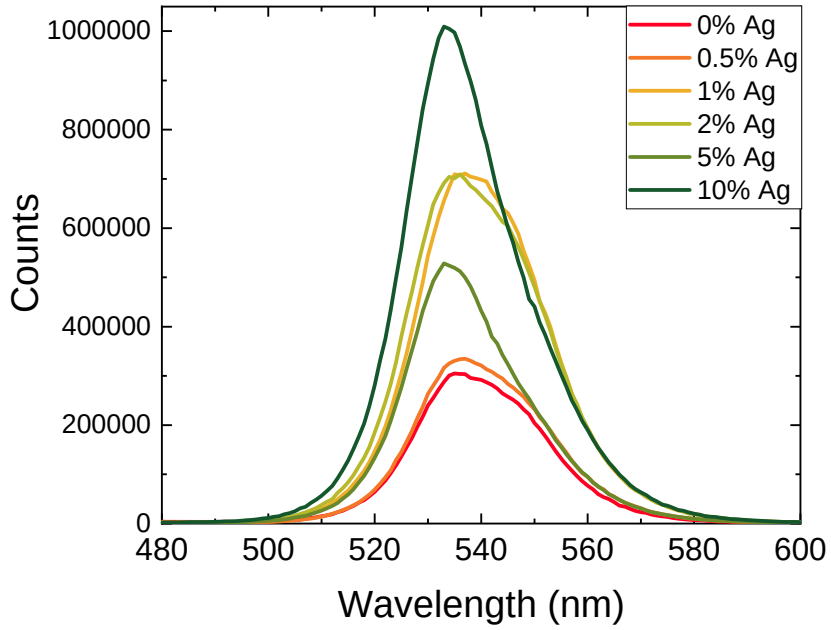

Figure S9. PL spectra from Figure 6a shown without normalization. Brightness increases as a function of Ag composition, with the majority of this increase attributed to increases in film thickness (see Figure S8).

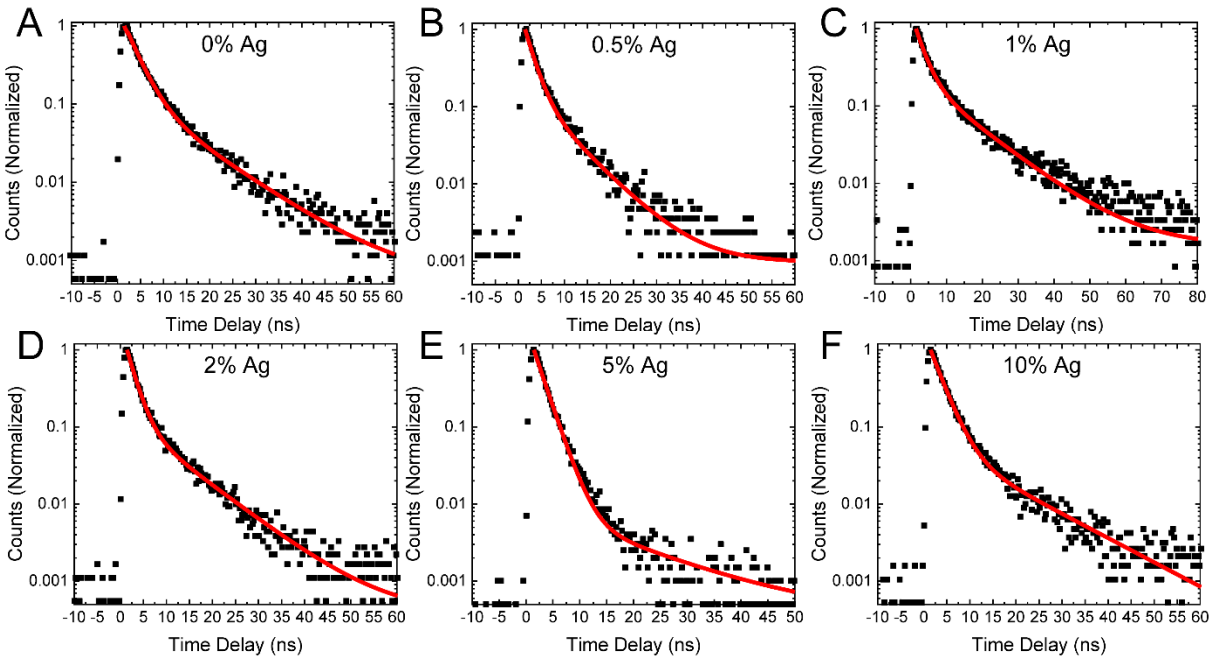

Figure S10. TRPL decay curves at 540 nm of MAPBr films on glass deposited with the addition of (A) 0%, (B) 0.5%, (C) 1%, (D) 2%, (E) 5%, and (F) 10% Ag^{+}. Data is in black squares and the fit curve is denoted by a red line. Data was fit to a biexponential decay function with parameters seen in Table 2.